

Scenarios and Economic Analysis of Fronthaul in 5G Optical Networks

Andrea Di Giglio, Annachiara Pagano

Abstract— This work presents a techno-economical comparison between different emerging architectural approaches for 5G networks: C-RAN, centralized, where a BBU hotel collects several fronthauling streams, able to meet challenging requirements imposed by emerging 5G technology and DA-RAN, considered as an evolution of C-RAN, where resources are disaggregated in order to satisfy the requirements of different applications. Main results, obtained by an analytical evaluation of the cost of a metropolitan area network, show that disaggregating the hardware and software radio access network brings architectural and functional advantages, able to better meet the bandwidth and latency requirements imposed by the 5G verticals.

Once analyzed the validness of the solution, we provide a cost analysis that firstly demonstrates that DA-RAN also brings economic advantages w.r.t. C-RAN.

Furthermore, observing that the predominant share of the cost of the solution is given by the fiber of the local loop, we evaluate the introduction of TWDM PON in this area in order to share the fiber and reduce the cost of the network.

Index Terms— 5G mobile communication, Cost benefit analysis, Optical fibers, TWDM PON, radio access network architecture.

I. INTRODUCTION

COMPATIBILITY with legacy (Long Term Evolution – LTE, and WiREless Fidelity - WiFi technologies), together with the improvement of spectral efficiency and throughput, represent essential requirements for 5G networks. To fulfill these requirements in a cost-efficient manner, operators evaluated the migration from the legacy Distributed Radio Access Network (D-RAN) paradigm, featured by co-location of Base Band Units (BBUs) and Remote Radio Heads (RRHs), towards the new Cloud/Centralized Radio Access Network (C-RAN). In the latter architecture, the BBU resources are pooled at a common central unit in an effort to reduce capital and operational expenditures, while remote RRHs are directly connected to the BBU pool through high bandwidth transport links, known as fronthaul. C-RAN

Manuscript received June 29th, 2018; revised XXXXXX. This work has received funding from the European Union's Horizon 2020 research and innovation programme under grant agreement No 762057 (5G-PICTURE).

Andrea Di Giglio and Annachiara Pagano are with TIM, Innovation department, Italy (e-mail: andrea.digiglio / annachiara.pagano@telecomitalia.it).

The authors would like to acknowledge Prof. Dimitra Simeonidu, Markos Anastasopoulos (University of Bristol), Prof. Anna Tzanakaki (University of Bristol, UK and National and Kapodistrian University of Athens, Greece), Marco Schiano (TIM). Special thanks Dr. Marjia Furdek and Liza Bromma for the review of the manuscript.

approach addresses some limitations of D-RAN, such as high costs of installation of complicate radio sites, as well as limited scalability and flexibility. On the other hand, C-RAN requires huge transport bandwidth and imposes strict latency and synchronization constraints [1], imposed by the timing requirement of Hybrid Automatic Retransmit reQuest (HARQ) protocol used as a retransmission mechanism between radio unit and eNodeB in an LTE network, maintained in 5G for compatibility reasons. The Horizon 2020 project 5G-PICTURE [2] proposes a novel architecture exploiting flexible functional splits to address the limitations of C-RAN. In the project approach the functional split can be flexibly decided, based on some factors such as transport and service requirements, finding the best splitting option able to satisfy the challenging requirements set by emerging “verticals”, for example high-speed train, automotive, and industry 4.0 [3-5].

II. NETWORK PARADIGM EVOLUTION

The operators' efforts to provide efficient and flexible fronthaul solutions while driving down the cost have been steering a continuous network evolution. The centralization of the base-band processing in C-RAN has been shown to reduce capital and operational costs by more than 30% [6-7] and to enable the implementation of advanced radio features such as Coordinated Multi-Point (CoMP) and beamforming. In addition the antenna sites are simplified with respect to D-RAN, since no base-band processing is required, allowing significant simplification in installation and maintenance, corresponding to Capital Expenditures (CapEx) and Operational Expenditures (OpEx) savings. However, C-RAN also introduces several disadvantages, since it requires huge bandwidth and ultra-low latency that make it unsuitable to satisfy 5G verticals requirements, especially when CPRI is adopted as fronthauling technology. In fact, CPRI is based on carrying time domain baseband I/Q samples between RRH and BBU. Thus, it needs a high capacity fronthaul, low latency, low delay variation and fine synchronization. To address this issue, references [8-9] propose a paradigm shift from C-RAN to a novel concept adopting the notion of disaggregation of hardware and software components across wireless, optical and compute/storage domains. This approach, referred to as “Dis-Aggregated RAN” (DA-RAN), allows decoupling of hardware and software components creating a common “pool of resources” that can be independently selected and allocated on demand, which comprises, in principle, any 5G service.

DA-RAN is a further evolution of Virtual RAN that is an architecture consisting of a centralized pool of baseband units (BBUs), virtualized RAN control functions and service delivery optimization. Compared with a virtual RAN, where baseband modules are moved away from the base station towards data centers [10], DA-RAN, spreading network functionalities across the network, offers enhanced scalability, upgradability and potential sustainability, particularly relevant to 5G, supporting huge and consistently growing number of devices and services.

In addition, references [8-9] show that this alternative RAN approach is designed for flexible functional splits between the BBU and the RRHs. DA-RAN introduces the need to develop new technology solutions both at the transport network segment, for the interconnection of the RRHs with the BBUs, and at the data centers level for the processing of BBU functions. For the transport network segment, references [8-9] consider a multi-technology architecture, comprising point-to-point microwave links and elastic optical network technologies.

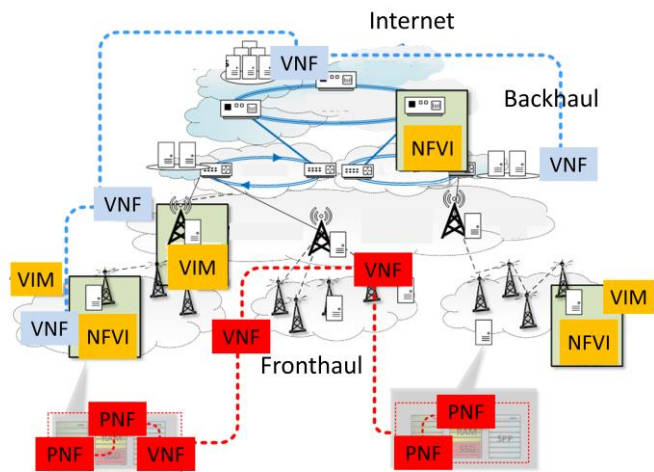


Fig. 1. DA-RAN network paradigm supporting integration of fronthauling and backhauling [2]

Fig. 1 depicts a scheme of the DA-RAN architecture, highlighting the concept of flexible RAN functional splits and the integration of fronthaul (FH) and backhaul (BH) on the same transport network. An important aspect of this architecture is the hardware programmability and the adoption of distributed Physical/Virtual Network Functions (PNFs/VNFs). These are handled by Virtualized Infrastructure Managers (VIM), responsible of controlling managing the Network Function Virtualization infrastructure (NFVI) compute, storage, and network resources, within the operator's infrastructure domain. FH and BH services are supported through a combination of PNFs and VNFs orchestrated by appropriate service chains.

III. QUANTITATIVE ANALYSIS

A. C-RAN and DA-RAN comparison for transport network

In this study we perform a set of network planning simulations on C-RAN and DA-RAN aimed at comparing

costs, energy consumption, and efficiency figures. A schematic view of the analyzed network is depicted in Fig. 2.

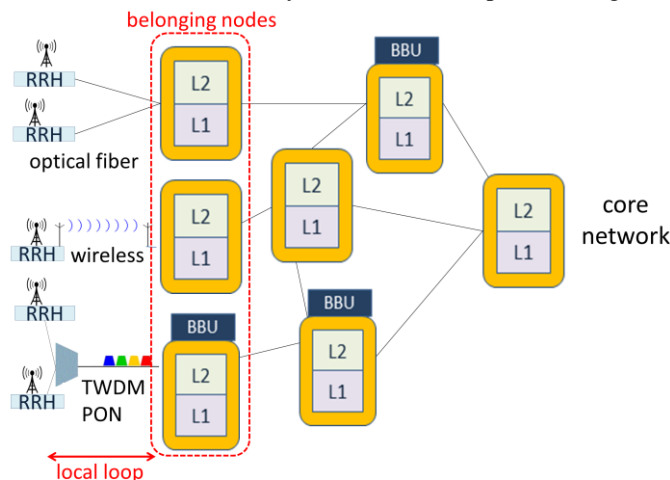


Fig. 2. Architecture of the network analyzed in the simulations

In the envisioned architecture, the connection between the radio site or, more precisely, the RRH, and the core network consists of a local loop and a connection in a meshed metropolitan network, as shown in Fig. 2.

The local loop, ranging from a few hundred meters to less than 10 km, consists of the link between the radio site and the first network node (referred to as the belonging node in the following). This segment can be based on point-to-point optical links equipped by grey transceivers or wireless connectivity. The belonging node grooms the traffic directed towards the same destination at layer 2, usually the baseband unit (BBU), and then splits the traffic into packet (L2) and optical (L1) services. L2 traffic is groomed with other traffic at intermediate nodes along the path to destination, whereas L1 optical circuits are directly delivered to the destination, optically bypassing intermediate nodes through Reconfigurable Optical Add Drop Multiplexers (ROADMs).

If the traffic demand between a pair of nodes exceeds a configurable threshold, the optical bypass is implemented; otherwise the traffic demand is routed at L2. In our study, we investigate different thresholds of L1/L2 traffic transmission.

Each node is equipped by both L2 and L1 optical switching functionality. L2 switching is fulfilled by MPLS-TP fabric (the throughput ranges between 1.6 Tbit/s and 19.2 Tbit/s), whereas L1 switching is implemented by a ROADM, consisting of low-cost wavelength selective switches based on silicon photonics. The nodes are equipped with 10, 40 and 100 Gbit/s optical transceivers, and the most cost-efficient option is selected for each lightpath.

The lightpaths are routed over a WDM system with 40 wavelengths per fiber, and are established using an heuristic Routing and Wavelength Assignment (RWA) algorithm, based on shortest path routing and first fit wavelength assignment.

All the costs simulations are provided over a simplified shape of a metro/regional area network (MAN) of northern Italy, with a very high user density distribution. It consists of rings interconnected by a meshed core network to the hub

nodes. Each ring connects a variable number of BBU sites and L1/L2 nodes. The MAN serves more than 1400 antenna sites. In the first part of the study, we consider point-to-point fiber connections between the antennas and their belonging nodes, with the exception of 80 sites, connected by mmWave radio links because they are placed in locations unreachable by fiber. In the second part, we consider Time Wavelength Division Multiplexing Passive Optical Networks (TWDM PON) in an effort to understand the economically advantages of this option compared to the point-to-point interconnection. In this case dynamic bandwidth allocation (DBA) algorithm is used in order to satisfy 5G latency and synchronization requirements.

Four areas inside the considered region are covered by small cells (about 300 antennas), offloading macro-cell traffic insisting on the same geographical region. The entire network serves more than 300.000 users and transports 940 Gbit/s whole bidirectional traffic in a mixed urban/rural area. Massive MIMO is also considered in some cases, about 10% of the total number of radio sites. This low percentage is justified by the rurality of the area. The assumed splitting option is transported by Common Public Radio Interface (CPRI) that guarantees the best performance for C-RAN. Despite of this splitting option allowing advanced functionalities, such as CoMP and beamforming, the associated CPRI stream strictly limits the maximum distance between RRH and BBU to 24 km [11], and requires a bitrate more than tenfold the end user bitrate, making it critical long geographical connections. In a 5G environment characterized by the bandwidth explosion required by the network verticals, the transport of CPRI will quickly become too restrictive. The new eCPRI [12], considered as an option in the following evaluation, overcomes some CPRI limitations. The chosen option for eCPRI is the transport of frequency domain I/Q symbols (split I_d/I_u), allowing more than 5-fold bandwidth saving in the fronthaul w.r.t. CPRI. The paper does not consider installation of infrastructure for new antennas, but we consider to use the same sites already used for 2G-3G-4G. The cost calculation is after a hypothetical complete substitution of 3G/4G traffic with 5G one, i.e. when 4G traffic will be neglectable or carried as 5G (virtual / DA-RAN).

TABLE I
ANALYZED CASE STUDIES

	Splitting option / transport	Optical bypass Threshold	Optical interfaces
1	Opt. 8 CPRI	45 Gbit/s	100 Gbit/s
2	Opt. 8 CPRI	8 Gbit/s	10/40/100 Gbit/s
3	I_d/I_u eCPRI	8 Gbit/s	10/40/100 Gbit/s

Table I reports the characteristics of the simulated use cases, i.e., the splitting option, the threshold to enable optical bypass and the adopted optical interfaces. For each use case, the C-RAN and the DA-RAN networks have been dimensioned and compared w.r.t. costs, energy consumption and dimensioning parameters.

The only difference between use case 1 and 2 is the usage of 100 Gbit/s interfaces only in use case 1, while use case 2 considers also 10 Gbit/s and 40 Gbit/s interfaces in order to optically transport smaller flows without any preventive electrical grooming. The fronthauling signal is the same for use cases 1 and 2, whilst use case 3 differs from the previous ones for the splitting option and the fronthauling transport technology, where Ethernet interfaces are adopted (eCPRI).

The simulations, carried out using a self-produced and non-commercial software, based on Microsoft Visual Basic, have as input the needs of the 5G user traffic (TIM internal estimates).

The first step is to convert user traffic into fronthauling traffic according to the adopted splitting option.

At this point we calculate the traffic matrix that loads the metropolitan network as the sum of the fronthauling traffic matrix (from belonging nodes to the reference vBBUs) and backhauling matrix (from the vBBUs to the 5G core-network). The next step is the sizing of the network elements (nodes and links) taking into account:

- Each node consists both of L2 fabric (able to aggregate traffic with the same destination) and L1 matrix
- Optical bypass is adopted over an established threshold
- Heuristic RWA algorithm is used for allocate wavelengths over the L1 transparent network
- Dijkstra algorithm is adopted for routing traffic
- 1:1 traffic protection is considered: working and protection are node disjointed paths.

Once the traffic is routed, the tool dimensions the network elements (links and nodes) and calculate the total costs and the total energy consumption.

Tables II and III report the cost of the entire network, expressed in XCU (1 XCU is the cost of grey 10G SFP Short Reach transceiver as available at the beginning of 2016), showing that the introduction of a splitting option alternative to CPRI (e.g. eCPRI, option 3) reduces costs and energy consumption, especially in the transport segment. The costs are reported as Yearly Total Cost of Ownership (YTCO), calculated as

$$YTCO = \sum_i \frac{CAPEX_i}{AP_i} + \sum_j OPEX_j \quad (1)$$

In (1), $CAPEX_i$ and $OPEX_j$ are the i-th and j-th components of CapEx and Operational Expenditures OpEx respectively. In order to harmonize the sum, each CapEx has to be annualized, distributing the investment over the appropriate amortization period (AP).

The cost of each individual component is the result of a complex work provided in 5G-Crosshaul project [13]. In this study the complete set of network elements has been valorized. Reference [13] reports, for instance, layer 2 fabrics costs ranging from 1.6T to 19.2T capacity and from 45.54 XCU to 1092.82 XCU. The document contains also the costs for L1 devices, interfaces and the energy consumption of components used in the evaluation reported below.

TABLE II
SYNTHESIS OF SIMULATION RESULTS FOR C-RAN

Option	YTCO	YTCO (without RRH)	Energy (MWh/year)	Max link size (parallel fibres)	Max nodal degree
1	14136.27	10839.59	2338.96	6	24
2	15856.17	12318.27	3475.73	6	24
3	11343.71	7631.99	2685.20	2	9

TABLE III
SYNTHESIS OF SIMULATION RESULTS FOR DA-RAN

Option	YTCO	YTCO (without RRH)	Energy (MWh/year)	Max link size (parallel fibres)	Max nodal degree
1	12992.15	9482.87	2403.002	5	17
2	14395.62	10827.64	3328.705	5	22
3	10369.47	7121.93	2617.37	1	8

Beside the cost calculation, we also evaluated the total energy consumption, summing the energy consumption of the single components (individual data from reference [13]), including the energy necessary for cooling. Finally, after link and node dimensioning, we evaluated the maximum link size, that is the number of parallel fibers necessary in the most loaded link, and the maximum nodal degree, that is the total number of fiber pairs connected to the node with the highest number of connections.

The comparison of figures in Tables II and III demonstrates that DA-RAN allows an economic saving, albeit of a minor extent. It is important to note that the maximum nodal degree is very high, in particular for CPRI splitting in C-RAN architecture. This imposes either a cumbersome ROADM node architecture with many interconnections, greatly increasing costs.

TABLE IV
DETAILS OF COSTS RESULTS FOR USE CASE 3
CAPEX (yearly cost)

	C-RAN	DA-RAN
TWDM PON	0.00	0.00
L2 matrix	170.11	162.37
10G interfaces	3.61	74.85
40G interfaces	31.32	39.69
100G interfaces	280.61	52.20
ROADM	102.41	97.89
Wireless	386.75	96.16
OPEX		
	C-RAN	DA-RAN
Energy	409.71	642.53
fiber network	730.22	102.65
fiber local loop	4934.34	4934.34
space (racks)	113.10	95.97
Maintenance	480.14	436.52

A more detailed analysis, reported in Table IV, makes clear that the most significant savings items allowed by DA-RAN

are the interfaces and the fiber in the network. In fact DA-RAN solution presents shorter fronthauling connections, due to the need to bring the basic bandwidth functionality closer to the customer and to the usage of fronthauling interfaces lighter than CPRI. This allows the use of smaller interfaces and less fiber in the meshed network (from the belonging node to the core network). On the other hand the fiber in the local loop is unchanged in the two compared solutions and it represents the most important cost share.

B. Economic analysis of local loop and introduction of TWDM PON

The conclusion of the first part of this paper, consolidating the results reported in [14], is that DA-RAN architecture allows the satisfaction of challenging requirements of 5G verticals (e.g. Smart Industry, Automotive, Mega Events, High Speed Trains, ...) in a more cost-efficient and scalable way than C-RAN. Nevertheless, an important share of the cost is the fiber for local loop. An idea to mitigate this cost is by introducing TWDM PON [15] in this segment. On the one hand, this allows fiber savings due to sharing of fibers by multiple radio sites, but, on the other hand, it requires the introduction of devices whose cost w.r.t. grey point-to-point short haul interfaces is significantly higher.

In order to reduce the cost of the local loop, the first step in this study is dedicated to define some basic rules for understanding under which conditions the adoption of TWDM PON is economically advantageous compared to point-to-point fiber connections. Based on this understanding, in the second step we analyze the most promising of the previous case studies, i.e., DA-RAN with eCPRI fronthauling interface, with TWDM PON adoption.

To compare the performance of the two solutions of interest, i.e. TWDM PON and point-to-point fiber, we perform a set of case studies with different geographical slicing solutions. In the studies, we vary the size of a circular crown identified by the distance from the belonging node (d_m is the mean distance and Δd the spread of distance w.r.t. the average) and the angle of the slice (see Fig. 3).

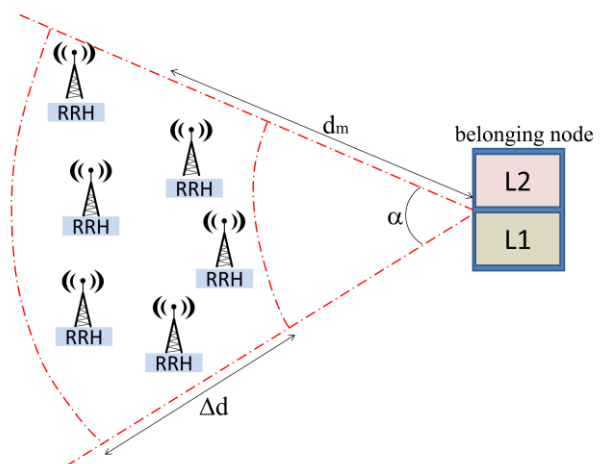


Fig. 3. Graphical representation of geographical slicing for TWDM PON / point-to-point cost comparison

A Monte Carlo method randomly distributes an established number (n) of sites (RRH) inside the circular crown slice. The RRHs inside the area defined by α , d_m and Δd are connected to the belonging node via (i) point-to-point fiber (Fig. 4) and (ii) TWDM PON (Fig. 5).

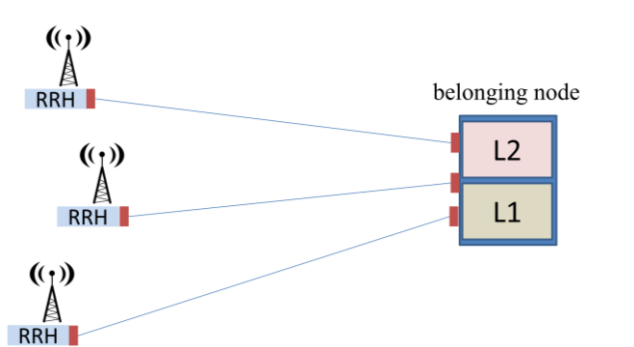


Fig. 4. Point-to-point connectivity between the RRHs and the belonging node

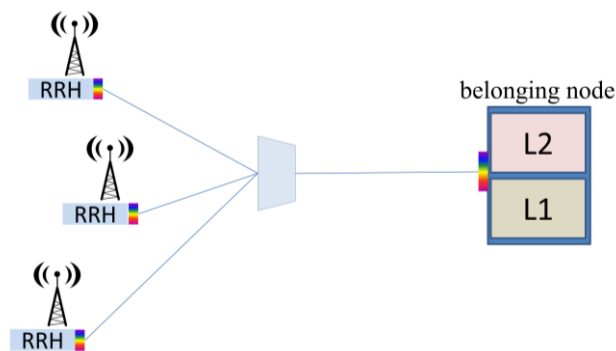


Fig. 5. TWDM PON between the RRHs and the belonging node

Figs. 4 and 5 show the evolution from the point-to-point solution, where cheap grey transceivers are adopted but a dedicated fiber between the radio site and the belonging node is installed, to the TWDM PON solution that allows fiber savings, but needs more expensive colored interfaces.

TABLE V
DETAILS OF COSTS POINT-TO-POINT AND TWDM PON SOLUTIONS

	point-to-point	TWDM PON
10 GE grey transceiver	0.611	----
ONT	----	0.893
Colored 10G transceiver (RRH)	----	1.786
Colored 10G transceiver (belonging node)	----	3.571
Splitter	----	0.286
100G interfaces	----	0.286
Yearly fiber rent (per km)	0.535	0.535

Table V reports the yearly costs of single elements (in XCUs) for the two solutions. These costs are derived from reference [13] and [16].

The cost savings introduced by TWDM PON are due to fiber sharing in the link between the splitter and the belonging

node. The location of the splitter influences the final cost because it fixes the shared section of the fiber. For our study, we tune the location of the splitter considering it as unconstrained because it can be positioned in any street manhole or cabinet that are ubiquitously distributed.

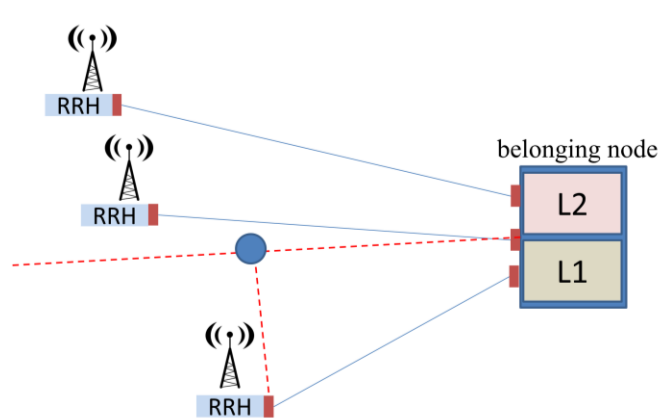


Fig. 6. Splitter location in the TWDM PON solution

The process of identifying the location of the splitting point is shown in Fig. 6 and described as follow:

- the line where the splitting point is located has an angle corresponding to the average of the angles of the RRHs w.r.t. belonging node.
- Once the line has been identified, the splitting point is identified as the projection on this line of the RRH closest to the belonging node

We perform several costs evaluations by comparing the TWDM PON and point-to-point fiber solutions in a set of case studies, by varying d_m from 3 to 9 km and Δd from small (3 km) to wide spread (9 km). The angle α of the slice is in the range between 60 degrees (partial coverage) and 180 degrees (full coverage).

The number of RRH sites collected by a single belonging node was also changed between 8 and 16 nodes taking into account the sharing of a TWDM PON carrier between two nearby RRHs.

Fig. 7 reports the number of connections where PON is advantageous with respect to PtP considering full coverage (180 degree slice aperture, that is the worst case) and small spread ($\Delta d = 3$ km), for a varying distance d_m and number of RRH sites per belonging node. For average distances longer than 4.5 km (the upper bound of the 3 km average distance column), TWDM PON is cheaper than point-to-point on more than 60% of connections as shown in Fig. 7.

Fixing a small spread and 6 km average distance ($\Delta d = 3$ km, $d_m = 6$ km), Fig. 8 shows that the TWDM PON is advantageous with respect to point-to-point solution for 90% of the connections for slice angles up to 120 degree, and for more than 50% of connections in case of uniform coverage (180 degree slice, 8 nodes).

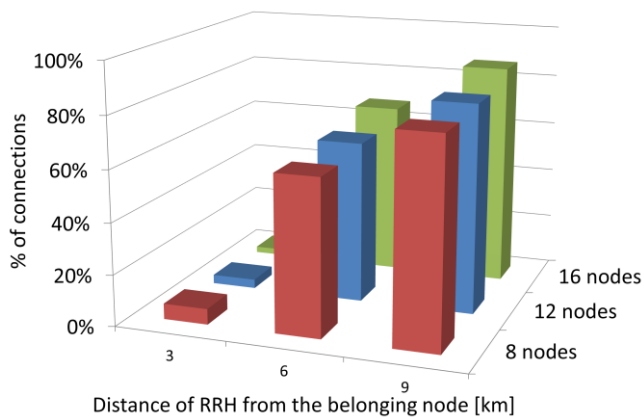


Fig. 7. Percentage on the number of connections where TWDM PON is advantageous with respect to point-to-point for different distance of RRH from the belonging node

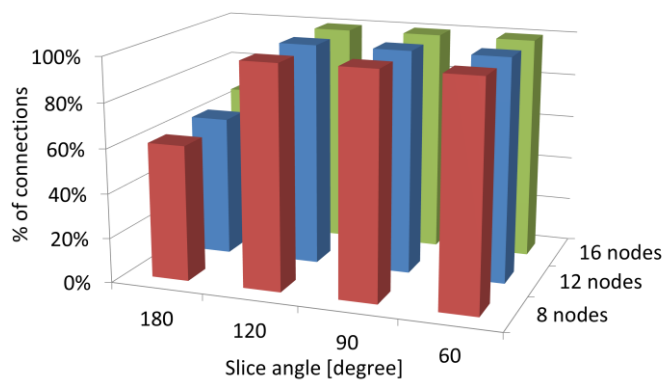


Fig. 8. Percentage on the number of connections where TWDM PON is advantageous with respect to point-to-point for different slice angles

In case of a uniform geographical distribution of RRHs, for distance greater than 7.5 km (maximum distance of 6 km average and 3 km spread), the TWDM PON advantage is enhanced by aggregating units in two different PON trees, each of them covering an area subtended by a 90 degrees angle, to better exploit fiber savings.

To summarize, the cost evaluations indicate that the introduction of TWDM PON instead of point-to-point fiber connections is advantageous in case when:

- The distance between the radio site and the belonging node is greater than 7.5 km, independently of the angular distribution of RRH.
- The distance between the radio site and the belonging node is greater than 4.5 km, but lower than 7.5 km. In this case the radio sites are groomed in the same TWDM PON, covering at maximum an angle of 90 degrees.

In our simulation, TWDM PON with 4 wavelengths and 8 Optical Network Terminations (ONTs) is used, where each ONT is connected to an RRH.

Following these rules, 1081 out of 1497 RRHs are connected to the belonging node via TWDM PON. 80 wireless connections remain, since some sites are unreachable via fiber (e.g., mountains, some small cells, etc.).

The simulation has been provided only for the eCPRI solution adopting DA-RAN (use case 3), as it is the only one

presenting fronthauling throughput needs compatible with the TWDM PON capacity.

The results are reported in Table VI. In option 3a, all the RRHs are connected via TWDM PON (except the 80 RRHs connected wireless), whereas in option 3b only the RRHs that satisfy the location rules identified in the previous paragraphs (1081 out of 1497) are attached via TWDM PON.

TABLE VI
SYNTHESIS OF SIMULATION RESULTS (ADOPTING TWDM PON)

	YTCO	YTCO (without RRH)	Energy (MWh/year)	Max link size (parallel fibres)	Max nodal degree
3a	11385.15	7982.41	2733.63	1	8
3b	9755.95	6353.21	2732.62	1	8

The part related to the metropolitan transport network is unchanged with respect to the option 3: the traffic to be transported is the same both in terms of endpoints and consistency (the traffic matrix of the transport network is the same for the case 3, 3a and 3b). Thus, the maximum number of parallel fibers on the same link and the maximum nodal degree is the same for case 3a and 3b and with respect to case 3.

The energy consumption is slightly greater than the case where point-to-point is adopted, due to a bigger consumption of TWDM PON transceivers w.r.t. a couple of grey interfaces.

The most interesting results are the ones regarding the costs. The yearly total cost of ownership of solution 3a is about 9% greater than solution 3 in Table III, demonstrating that the widespread usage of TWDM PON in the access segment might not be the cheapest solution.

On the contrary, substituting point-to-point fiber with TWDM PON in line with the guidelines resulting from the simulation reported above, the cost saving is more than 6% considering the total cost of ownership of the entire network, and more than 11% excluding the RRHs cost from the computation, again comparing figures with data in Table III.

Table VII presents a detailed cost break-down of the use cases 3 and 3b. The most evident trend is that the higher expenditures for TWDM PON equipment (1166 XCUs) are counterbalanced by savings in the local loop fiber of 2109 XCUs.

TABLE VII
DETAILS OF COSTS RESULTS FOR USE CASES DA-RAN (3 AND 3B)

	CAPEX (yearly cost)	
	Use case 3b (point-to-point mixed with TWDM PON)	Use case 3 (point-to-point)
TWDM PON	1165.94	0.00
L2 matrix	168.84	162.37
10G interfaces	76.06	74.85
40G interfaces	30.67	39.69
100G interfaces	54.81	52.20
ROADM	97.89	97.89
Wireless	96.16	96.16

OPEX		
	Use case 3b (point-to-point mixed with TWDM PON)	Use case 3 (point-to-point)
Energy	663.40	345.19
fiber network	102.65	102.65
fiber local loop	2731.94	4934.34
space (racks)	95.97	95.97
maintenance	682.13	436.52

IV. CONCLUSIONS

5G-PICTURE project designed the DA-RAN architecture to comply with the new 5G verticals' stringent requirements. In this work, we demonstrated that DA-RAN approach also allows cost and energy savings and a better traffic distribution in the optical fronthaul network.

Adopting point-to-point fiber connections between the radio site and the closest node of the metropolitan transport network (local loop) is not worth it, representing just under half of the total annual cost. A way to reduce this cost is the introduction of TWDM PON in the local loop, allowing fiber sharing. Despite fiber savings, there is an additional cost for TWDM PON equipment, not present in the point-to-point solution. We performed a study to establish under which conditions it might be advantageous to replace the point-to-point with the TWDM PON. We demonstrated that the introduction of TWDM PON is beneficial to connect the RRHs furthest from the belonging node. The completed simulation showed that the usage of TWDM PON under certain conditions can lead to quantifiable economic benefits of around 10%. Further savings can be exploited by sharing the TWDM PON optical distribution network fiber infrastructure also with the residential traffic running over legacy G-PON and XGS-PON.

REFERENCES

- [1] D. Bladsjo et al., "Synchronization aspects in LTE Small Cells," IEEE Comm. Mag., vol.51, no.9, pp.70,77, Sep. 2013
- [2] 5G-PICTURE, <http://www.5g-picture-project.eu/index.html>
- [3] U. Dötsch et al., Quantitative Analysis of Split Base Station Processing and Determination of Advantageous Architectures for LTE, Bell
- [4] D. Wubben et al., "Benefits and Impact of Cloud Computing on 5G Signal Processing: Flexible centralization through cloud-RAN," IEEE Signal Processing Magazine, vol.31, no.6, pp.35-44, Nov. 2014.
- [5] A. Tzanakaki, "Wireless-Optical Network Convergence: Enabling the 5G Architecture to Support Operational and End-User Services", IEEE Commun. Magazine, 55 (10), 184-192, 2017
- [6] C. Raack et al., "Centralised versus Distributed Radio Access Networks: Wireless integration into Long Reach Passive Optical Networks", Conference of Telecommunication, Media and Internet Techno-Economics (CTTE), Nov. 2015
- [7] A. De La Oliva et al., "Final 5G-Crosshaul system design and economic analysis", 5G-Crosshaul public deliverable, Dec. 2017
- [8] A. Tzanakaki, M. Anastasopoulos, and D. Simeonidou, "Converged Access/Metro Infrastructures for 5G services", OFC 2018, invited
- [9] N. Gkatzios, M. Anastasopoulos, A. Tzanakaki, and D. Simeonidou, "Compute Resource Disaggregation: An Enabler for Efficient 5G RAN Software", EuCNC 2018
- [10] N. Cranford, "What is a Virtual RAN" <https://www.rcrwireless.com/20180323/what-is-a-virtual-ran-tag27-tag99>, Mar. 2018
- [11] H. J. Son et al., "Fronthaul Size: Calculation of maximum distance between RRH and BBU", NETMANIAS, Apr. 2014

- [12] eCPRI, "V1.0 Common Public Radio Interface: eCPRI Interface Specification," Ericsson AB, Huawei Technologies Co. Ltd, NEC Corporation and Nokia, Aug. 2017
- [13] 5G-Crosshaul, "D1.2: Final 5G-Crosshaul system design and economic analysis", Dec. 2017
- [14] A. Di Giglio, A. Tzanakaki and D. Simeonidu, "Scenarios and Economic Analysis of Fronthaul" presented at the Optical Networking and Communication Conference & Exhibition, San Diego, USA, Mar. 12-15, 2018.
- [15] ITU-T G.989.x Series of Recommendations "40-Gigabit-capable passive optical networks (NG-PON2)"
- [16] "Cisco Global Price List 2016," [Online]. Available: <http://www.scan25.com/index.php?search=SEF-10G-SR>.

Andrea Di Giglio received a Dr. Ing. degree in Electronic Engineering from the University of Pisa (Italy) and the Engineering License degree from Scuola S. Anna. He joined Telecom Italia Innovation Group in 1999.

The fields of his research are addressed toward Internet Security, Storage Area Networks and Optical Networks Architecture. He was involved in EURESCOM and European Projects on IP over optical networks; he was involved in the architectural Work Package of the IST Project Nobel (Phase 1 and 2) "Next generation Optical networks for Broadband European Leadership" as Work Package leader, and ICT STRONGEST as project coordinator.

Dr. Di Giglio is the author of dozens of publications, including books, conference papers and workshops.

Annachiara Pagano obtained her Master Degree in Physics at the University of Torino. She has been working with Telecom Italia (formerly CSELT) since 1994. Her fields of interest are high capacity optical networks, focusing on network design and testing. She has been involved in several European projects (BOOM, GALACTICO; IDEALIST, PANTHER, ORCHESTRA and now 5G PHOS). She is now in the wireline access innovation group in TIM, and her main interest are TWDM and high speed PON, together with 5G fronthauling.

Dr. Pagano has authored and co-authored more than fifty technical publications covering design and testing aspects of optical components and systems.